U.S. Department of the Interior
U.S. Geological Survey

GEOPHYSICAL LOGS AND GROUNDWATER CHEMISTRY IN THE A/M AREA, FINAL REPORT, SAVANNAH RIVER SITE, SOUTH CAROLINA

Philip H. Nelson[1] and Joyce E. Kibler[1]

Open-File Report 96-75

This report is preliminary and has not been reviewed for conformity with U.S. Geological Survey editorial standards. Any use of trade names is for descriptive purposes only and does not imply endorsement by the USGS. This work was supported by the Department of Energy under Interagency Agreement DE-AI09-91 SR18222.

1996

1. U.S. Geological Survey
Denver, Colorado

TABLE OF CONTENTS

List of Tables

List of Figures

List of Plates

In Pocket: Digital data on three 3.5-inch diskettes for IBM-compatible personal computers: Logs from 41 wells, as listed in Tables 2 and 3, and from 28 penetrometer runs listed in Table 4.

SUMMARY

Electrical resistivity logs acquired in the A/M area with short (16-inch) and long (64-inch) normal resistivity tools have been compensated for the resistivity of the borehole fluid and for hole size. Segments where the measurements were off-scale or unduly noisy have been nulled. Gamma-ray logs have been smoothed to reduce statistical noise. The resulting logs are plotted in groups and on sections and are made available on diskettes.

The electrical resistivity logs exhibit a negative resistivity gradient: the resistivity at the water table is on the order of 1000 ohm-m and over a depth range of 25 to 60 feet decreases roughly an order of magnitude. The gradient occurs in both the penetrometer logs and the well logs. It occurs in two wells immediately west of building 321-M. The gradient extends at least 4000 feet southwest of the Settling Basin, 1400 feet to the west, and 1000 feet to the east, and is unbounded in these directions. It also extends about 800 feet to the northeast of the Settling Basin, where its boundary is well defined within the MHT-series of wells.

Analysis of water samples shows that abundance of nitrate ion correlates with water conductivity. Reductions in water resistivity due to elevated nitrate concentration are compatible, through Archie's law, with reductions of formation resistivity observed in the resistivity logs.

This observed gradient could be caused by an increase with depth either in the occurrence of smectite or in the nitrate concentration in groundwater. If smectite can be eliminated as a factor in controlling rock resistivity, then electrical resistivity can be used to track a nitrate plume in the A/M area. An association between nitrate ion and the concentration of chlorinated solvents suggests that mapping of electrical properties might also lend insight into the migration pathways or even the distribution of chlorinated solvents.

INTRODUCTION

The Savannah River Site, located near Aiken, South Carolina, is operated by the U.S. Department of Energy. The A/M area at the site is undergoing characterization and pilot remediation work to locate and recover chlorinated solvents which were released to the subsurface. As part of this characterization effort, subsurface data have been obtained from water samples, from core measurements, by geophysical logging of boreholes, and by cone penetrometer runs. This report describes the second phase of a synthesis and study of existing geophysical logs and penetrometer runs in the A/M Area at the Savannah River Site. The first phase was reported in an interim report by Nelson and Kibler (1995); this final report draws heavily upon the data and observations of that document. The interim report accomplished three tasks: it examined groundwater electrical conductivity in terms of groundwater chemistry, it compiled the existing log

and core data into a coherent data base, and it described a method for computing porosity and water content in the unsaturated (vadose) zone.

This second and final report uses the compiled data base to examine further an intriguing association between groundwater chemistry and conductivity. Groundwater samples collected from screened wells within different aquifers and confining zones showed a good correlation between nitrate ion concentration and fluid conductivity, and a fair correlation between nitrate ion and concentration of chlorinated solvents. These two associations suggest that mapping of electrical properties may delineate the distribution of nitrate-rich water and thereby might also lend insight into the migration pathways or even the distribution of contaminants. In addition, resistivity logs from the cone penetrometer runs provided an intriguing pattern when grouped by sub-areas (Figure 26 of Nelson and Kibler, 1995). Runs from the south and to a lesser extent from the west of the Settling Basin showed negative resistivity gradients commencing above the water table and persisting to the total depth of the runs. Runs from the north of the Settling Basin showed little or no such gradient. Thus these resistivity logs from penetrometer runs can be grouped by area; these areas may indicate the direction of migration of nitrate-rich water which originated from the disposal of nitric acid into the Settling Basin.

To investigate further the resistivity behavior noted on the penetrometer runs, we have processed, plotted, and examined the electrical resistivity logs from the wells in the A/M area. Processing consists of correcting for the resistivity of the wellbore fluid and for wellbore diameter. The processed logs are plotted in Plates 1-7. Examination of the plots substantiates and extends the initial finding that a resistivity gradient exists in the subsurface in the area surrounding the Settling Basin. A simple model for the variation of resistivity with nitrate content is consistent with the observed gradient.

The wells and penetrations which have electrical logs are shown in a series of maps in Figures 1-3. The maps are similar to Figures 13-15 of Nelson and Kibler, 1995, which display all wells and penetrations having any type of log data. A fourth map (Figure 4) shows how the wells and penetrations are grouped with respect to the Plates. The first five Plates display all electrical logs from wells and penetrations without redundancy in five groupings. Plates 6 and 7 display selected wells and penetrations along two sections. Tables 2-4 list the penetrometer runs and the wells, giving the location and the Plates in which data are displayed. The digital data are available on diskette (in pocket).

PROCESSING AND CHARACTERISTICS OF LOGS

Processing of gamma-ray logs. Gamma-ray logs were smoothed with an eleven-point filter to reduce the fluctuations which were judged to be non-repeatable, that is, caused by inadequate

counting statistics. The eleven-point filter is a triangular filter with weights normalized to 1.0. The filter computes a weighted average which includes the central point and five points above and below the central point. Because the logs were digitized at 10 points per foot, a length of log equal to 1.1 feet is smoothed to create the output at each sample point. An example of this filtering procedure is shown in Figure 5.

Processing of electrical resistivity logs. The 16-inch and 64-inch normal resistivity logs were processed to remove the effect of the borehole fluid. If the resistivity of the borehole fluid matches the resistivity of the rock, then no correction is necessary. However, if the borehole fluid is less resistive than the rock, then current flows preferentially within the hole rather than into the rock, resulting in an apparent resistivity value which is greater than that of the rock. Conversely, if the fluid is more resistive than the rock, current flows preferentially into the rock, resulting in an apparent resistivity less than that of the rock. A graphical method for correcting for this effect was published by Schlumberger (1949) and automated by Scott (1978). We use Scott's algorithm to correct the logs.

To correct a resistivity log, the algorithm requires three parameters: the tool diameter (which is 2.5 inches), the hole diameter, and the borehole fluid resistivity. The hole diameter was taken from the caliper log if one was available, or else the bit diameter was used. The fluid resistivity was taken to be 17.7 ohm-m, based upon an average of measurements made with a fluid resistivity tool in four MHT-wells.

Examples of the correction are shown in Figures 6a and 6b. In the 12-inch hole (Figure 6a), the correction reduces the value of the 64-inch measurement and increases the value of the 16-inch measurement, with the corrections being comparable at a depth of 150 feet. In the 5-inch hole (Figure 6b), the correction reduces the value of both the 16-inch and 64-inch measurements, but the reduction is greater for the 64-inch than for the 16-inch measurement (depth of 175 feet). The differences between the sense and magnitude of the corrections at comparable resistivity values in these two examples is due to the different hole sizes. Over the depth intervals shown in these two holes, the correction causes the 64-inch log values to be closer to the 16-inch log, that is, the separation between the two is reduced. This result is considered realistic and desirable in the absence of invasion effects because both logs should measure comparable resistivity values where the rock formation is relatively homogeneous (free of layers). The fluid resistivity probably varied through the course of the drilling program, but without records of the resistivity of the drilling fluid for each hole, correct values for each hole were not available. An average value of 17.7 ohm-m was used as the fluid resistivity in all the wells.

Resistivity from normal (two-electrode) resistivity logs. Two-electrode resistivity arrays were among the first borehole electrical tools. Spacings of 16 inches (called the short normal) and 64 inches (long normal) are standard spacings in both petroleum and groundwater logging systems. A

single potential electrode measures the voltage relative to a remote reference, in the presence of a single current electrode. The voltage-to-current ratio (in ohms) is converted to an apparent resistivity value (in ohm-m) by multiplication by a geometric factor (in m) appropriate to the array. More detail on tool operation and insight into tool response is available in texts such as Hearst and Nelson (1985).

In order for a two-electrode array to detect a thin resistive bed, both electrodes must be within the bed. In other words, the bed thickness must be greater than the electrode spacing. Thus the 16-inch array will respond to a resistive bed which is two feet thick but not to a one-foot bed. This response issue is illustrated in Figure 7 where the first two cases show that the response to a thin resistive bed is suppressed to a value less than that of the surrounding beds. This occurs because the resistive bed acts as a shield, deflecting current flow away from the potential electrode. With both electrodes within a thick resistive bed such deflection cannot occur, and the response increases although not to the full value of the bed resistivity (case 3 in Figure 7).

On the other hand, there is no comparable problem in detecting thin conductive beds. A low resistivity results when the electrodes straddle the conductive bed (Figure 8). Moreover, the apparent resistivity recorded in a thick conductive bed is closer to the true bed resistivity than it is in a thick resistive bed (compare case 4 to case 3 of Figure 7).

With these models in mind, it is easier to interpret the electrical logs pictured in the Plates. For example, the logs at 260 feet depth (125 feet elevation) in MSB-66TA (Plates 1 and 7) indicate a conductive bed coincident with the gamma-ray peak. The bed boundaries delineated by the 16-inch log match the gamma-ray bed boundaries while the 64-inch log indicates a wider bed. This discrepancy corresponds to case 4 in Figure 7 and occurs because of the greater spacing of the 64-inch array. The apparent resistivity value of the 16-inch log is less than that of the 64-inch log; this occurs because the bed appears thicker to the shorter array and hence the measurement approaches the true value more closely than does that of the longer array. Thus in general, inspection of the logs on the Plates shows that the 64-inch log appears more subdued, that is, beds appear thicker and maxima and minima are reduced compared to those on the 16-inch logs.

Comparisons among different electrical tools regarding bed resolution have been made previously (p. 30 of Nelson and Kibler, 1995). They are easily revisited here. Logs from CPT-1 and MSB-26AA (Plate 2), which are 200 feet apart, provide an excellent comparison regarding resolution. At 46 and 60 feet depth in MSB-26AA, the normal logs give just a hint of conductive beds which are much better defined by the cone penetrometer log at the same elevations.

Resistivity from the cone penetrometer. The cone penetrometer uses a four-electrode system called the Wenner array, in which current is transmitted between two outer electrodes and the

potential is measured by two inner electrodes. Spacing between each electrode is one inch. The Wenner array was devised for surface surveying and is not typically used in borehole logging. Figure 9 shows one of the few examples in the literature of the response to a Wenner array in the subsurface. In this example, which omits the borehole, the overall length of the array, as pictured in the figure, is exactly equal to the thickness of the resistive bed, which is 9 times more resistive than the surrounding shoulder beds. In this case, the highest apparent resistivity measured within the bed is about one-half that of the bed itself, and there is a deceptive minimum produced in the center of the bed. The lesson here is that the Wenner arrangement, like any electrode array, produces a response which is different from the true resistivity when the array size is comparable to the thickness of the bed. To see these effects with a one-inch array size, the data must be digitized at increments less than one inch. Coarser sampling results in aliasing which can cause spurious peaks to occur in the log.

An obvious advantage of the Wenner array is that it produces a symmetric response to a layer, with the spacing between inflection points approximating the bed thickness. Thus bed thickness is well defined by the array and the true resistivity is well defined by the apparent resistivity when the bed is sufficiently thick, on the order of twice the array size (8 inches).

Aside from the array characteristics, one must consider the effects of compaction exerted by the cone penetrometer upon the formation. Instead of removing material, the penetrometer displaces it, so the resistivity measurement is made in a compacted zone in which the porosity immediately surrounding the probe is reduced. In addition to compaction, the water in the soil must be mobilized as the probe enters. If the soil is saturated, it will remain saturated as it is displaced, and the effect of the probe penetration upon resistivity will be limited to that of pore volume reduction (compaction). In this case resistivity should increase with respect to the undisturbed condition. On the other hand, if the soil is unsaturated, the resistivity in the small volume around the probe will change in response to both the change in pore volume and the altered saturation conditions. In this case it is difficult to anticipate whether the resistivity will increase or decrease. The presence of clay minerals further complicates the effect of compaction.

ELECTRICAL LOG RESPONSE ACROSS THE A/M AREA

The electrical logs in Plates 1-7 can be inspected for effects of groundwater contamination from nitrate. Before doing so, we establish a model based upon analysis of water samples to ascertain what factors can cause a downward decrease in resistivity.

Archie's law can be used to relate rock resistivity R_0, water resistivity R_w, porosity ϕ, and cementation exponent m,

$$R_0/R_w = \phi^{-m}$$

for example, for $\phi = 0.4$,

$$R_0/R_w = 0.4^{-1.5} = 3.95, \text{ for } m = 1.5$$

$$R_0/R_w = 0.4^{-2} = 6.25, \text{ for } m = 2.0$$

Inspection of figures 21-24 of Nelson and Kibler (1995) indicates that porosity varies between 0.4 and 0.5 over the 60 feet penetrated below the water table; sample calculations in Table 1 are for these two values of porosity. As no measurements for m are available, computations have been carried out for values of 1.5 and 2.0. A value of $m = 1.5$ is reasonable for poorly consolidated sediments and a value of 2.0 is reasonable for consolidated sediments. The fluid conductivity, C_w, of water samples recovered from well screens ranges from 20 to 250 μS/cm as nitrate concentration ranges from near-zero to 25 mg/L (Fig. 3 of Nelson and Kibler, 1995). Corresponding values of R_w of 500 and 40 ohm-m are obtained using the conversion R_w (ohm-m) = 10,000 / C_w (μS/cm) (see footnote on p. 8 of Nelson and Kibler, 1985). The bounding values for R_0 given in Table 1 are determined by multiplying R_w by the factor determined from Archie's law (3.95 for $m = 1.5$ and $\phi = 0.4$, for example).

Table 1. Limiting values of rock resistivity R_0 for two values of fluid conductivity, C_w, two values of cementation exponent, m, and two values of porosity, ϕ.

	C_w (μS/cm)	R_w (ohm-m)	Porosity	R_0 (ohm-m) m = 1.5	R_0 (ohm-m) m = 2.0
fresh water	20	500	0.4	1976	3125
high-nitrate water	250	40	0.4	158	250
fresh water	20	500	0.5	1414	2000
high-nitrate water	250	40	0.5	113	160

Four factors can cause a decrease of R_o with depth: an increase of porosity, a decrease in m, an increase in clay content, or a decrease of R_w. Three of these four factors are explicit in Archies' rule. As already mentioned, an increase in porosity with depth has not been observed in

the available logs, and the variations (as opposed to trends) in porosity are modest (Table 1). In addition, sustained increases of porosity with increasing depth are considered unlikely due to compaction. The exponent *m* does not usually vary much within a formation, and if it were to vary, it would be expected to increase with depth, not decrease. These considerations reduce the liklihood that trends in either ϕ or *m* cause a negative gradient in resistivity.

The possibility of an effect from changes in clay content is another matter. The value of 500 ohm-m for R_w in Table 1 is quite high for groundwater. It is based upon samples taken by pumping from wells in the A/M area. By contrast, the value of 17.7 ohm-m used to correct the logs (see section "processing of electrical resistivity logs") represents the water used for drilling and can be expected to be less resistive than connate water. The more resistive samples normally encountered in surface and groundwaters are around 200 ohm-m (Hem, 1992, p. 69). Values of 200 ohm-m have also been reported from two wells in South Carolina, one at the Savannah River Site and another at Williston (Faye and Smith, 1994, p. 14). Thus, values of 500 ohm-m, corresponding to 20 μS/cm reported in samples from 7 wells in the A/M Area (Nelson and Kibler, 1995, p. 12), are a factor of 2.5 more resistive than the highest values reported elsewhere. At these high resistivity values of water, the estimates of Table 1 for R_0 will err on the high side because surface conduction will augment the flow of electrical current in the pore space. Archie's law is valid in clay-free sand. The higher the value of R_w, the more likely it is that the value of R_0/R_w will be lowered by the presence of clay minerals (see figure 5-11 of Hearst and Nelson, 1985). Even small amounts of clay, on the order of 1%, can be expected to reduce bulk rock resistivity below the values shown in Table 1.

The third control, R_w, is treated explicitly in Table 1, based upon water sample measurements. If the resistivity logs, which measure R_o, are in fact responding to R_w, then the logs may be used to track nitrate concentration.

With these controls in mind, the hypothetical log of Figure 10 can be inspected. It is based upon the values of R_0 given in Table 1 and illustrates how an electrical resistivity log in a clean sand might behave as it encounters fresh water at the top of a section and high-nitrate water at the bottom. Examination of the logs in the Plates shows that the resistivity gradients in many of the holes and penetrations to the south and west of the Settling Basin resemble the hypothetical log. Penetration CPT-7 (Plate 5) and well MHT-18C (Plate 3) provide good examples for comparison. Most of the logs display less than the order-of-magnitude decrease in resistivity indicated by Table 1 and Figure 10. Lesser fluctuations superposed upon the resistivity decrease reflect local variations in porosity, clay content, and possibly in the exponent *m*.

The character of the negative resistivity gradient within the MHT-series of wells (Plate 3)

is of particular interest because of the close spacing of the wells and the uniformity of the logging program. The gradient exists in the southern wells, MHT-17C through MHT-3C, but not in the northern wells, MHT-4C through MHT-10C. This mapping is supported by the two penetrometer logs; the gradient is present in CPT-19a but absent in CPT-15a (Plate 4 and Figure 11). The negative gradient increases to the south, that is, resistivity decreases with depth more rapidly in MHT-17C than in MHT-2C or 3C. Incidentally, the northern wells have a pronounced resistivity low at roughly 100 feet subsurface, ranging in thickness from 8 to 15 feet. The southern MHT wells do not have a comparable resistivity low. The physical properties of this zone, referred to as the "tan clay", have been discussed in terms of possible mineralogical compositions (p. 29 of Nelson and Kibler, 1995). Thus in the northern MHT-wells we observe the presence of the low-resistivity tan clay and the absence of a resistivity gradient below the water table, whereas in the southern MHT-wells we observe the converse situation. From the grain size data and gamma logs, it appears that the tan clay is not present in the southern MHT wells; certainly its low resistivity characteristic is absent from wells south of MHT-3C. If the resistivity gradient does in fact reflect the presence of nitrate-rich groundwater, then the tan clay could be influencing its disposition by blocking downward migration of contaminants.

With these results in hand from the MHT-area, where the resistivity gradient is well defined and possesses a clear boundary, we proceed to select all wells and penetrations having such a gradient. The results are shown in map form in Figure 12. The gradient extends 4000 feet southwest of the Settling Basin, 1400 feet to the west, and 1000 feet to the east. Due to lack of wells or penetrations beyond these limits, the full areal extent of the gradient is not defined. In Figure 12, the gradient is shown to exist in well MSB-75B but not in MSB-72B, although the interpretations are questionable in both these wells. The MSB-wells in the northeast area of the map completely lack any indication of the resistivity gradient (Plate 1). Two wells, MSB-23TAR and MSB-26AA, just west of Building 321-M, both display a clear resistivity gradient. Further west, four penetrometer runs (CPT-4, -3, -14, -23b in Plate 2) display a hint of a resistivity gradient, but because the gradient is more subtle than in the CPT runs to the south, the symbols for these four runs are not shaded in Figure 12.

However, it is possible that the resistivity gradient is caused by an increase in smectite content with depth below the water table. Smectite has high cation exchange capacity, roughly an order-of-magnitude greater than kaolinite (Table 6 of Nelson and Kibler, 1995). Small volume fractions of smectite can readily reduce the rock resistivity. Horton (1995) reported smectite in 9 of 22 samples and Segall (U. South Carolina, 1992, p. 29) reported smectite at depths below 170 feet. Thus, the possibility of a gradient in smectite content must be considered. Detailed analyis of clays in one or more of the wells where a resistivity gradient is prominent would be a good check at to whether conductive clay minerals are causing or otherwise influencing the resistivity logs.

In summary, the resistivity gradient is unambiguously absent in the MSB-wells to the northeast. It is unambiguously present to the southwest and immediately to the north of the Settling Basin. It is tempting to ascribe the negative resistivity gradient to the presence of a gradient in groundwater conductivity caused by nitrate ion concentration, and to assume that the absence of the gradient indicates the absence of nitrate ion. If this association is valid, and the competing hypothesis of smectite abundance is not, then the electrical resistivity structure can be used to track the nitrate plume. Resistivity values below the water table are sufficiently low that an induction tool can be used to re-log the existing wells. (Induction tools work well at low resisitivity, but are not reliable at resistivity values greater than 200 ohm-m). Induction tools can be operated in wells cased with PVC. However, small diameter induction tools may have limitations in the large diameter (12-inch) wells; the depth of investigation of the tool should be investigated before re-logging the wells. If the resistivity gradient does indeed reflect the migration of a nitrate plume, then re-logging the wells should show ephemeral changes in the resistivity logs reflecting the further progress or dispersion of the plume since the last logs were run (logging dates are given in Tables A1, A2, and A5 of Nelson and Kibler, 1995). By way of reference, DeSimone and Barlow (1985) and Church and Friesz (1985) have conducted successful applications of time-lapse induction logging to track the migration of contaminant plumes in shallow aquifers.

RECOMMENDATIONS

1. Analyze clay mineralogy in one or more wells where the resistivity gradient occurs to see if conductive clays (smectite) are causing or contributing to the negative resistivity gradient.

2. If clays are not significantly reducing the rock resistivity, design and field an induction log survey in cased wells to determine what changes have occurred in the resistivity profiles since the last date of logging. Include a neutron log, which will also work in a cased hole, and will provide information on changes in porosity and clay content.

REFERENCES

Church, P.E. and Friesz, P.J., 1995, Delineation of a road-salt plume in ground water, and traveltime measurements for estimating hydraulic conductivity by use of borehole-induction logs, paper Y in Proc. 5th Symposium, Minerals and Geotechnical Logging Society (Soc. of Prof. Well Log Analysts).

DeSimone, L.A, and Barlow, P.M., 1995, Borehole induction logging for delineation of a septage-effluent contaminant plume in glacial outwash, Cape Cod, Massachusetts, paper X in Proc. 5th Symposium, Minerals and Geotechnical Logging Society (Soc. of Prof. Well Log Analysts).

Faye, R.E., and Smith, W.G., 1994, Relations of borehole resistivity to the horizontal hydraulic conductivity and dissolved-solids concentration in water of clastic Coastal Plain aquifers in the Southeastern United States, U.S. Geological Survey Water-Supply Paper 2414, 33 p.

Guyod, H., 1944, Electrical well logging, Oil Weekly, August-December, series of 16 articles.

Hearst, J.R, and Nelson, P.H., 1985, Well logging for physical properties, McGraw-Hill Co.

Hem, J.D., 1992, Study and interpretation of the chemical characteristics of natural water, U.S. Geological Survey Water-Supply Paper 2254, 264 p.

Horton, R., 1995, X-ray diffraction studies of selected core samples from A/M area, Savannah River Site, South Carolina, USGS Open-file Report, 26p.

Nelson, P.H., and Kibler, J.E., 1995, Geophysical logs and groundwater chemistry in the A/M Area, Interim Report, Savannah River Site, South Carolina, U.S. Geological Survey Open-File Report 95-507, 68 p.

Schlumberger, 1955, Resistivity departure curves (Beds of infinite thickness), Document 7.

Scott, J.H., 1978, A Fortran algorithm for correcting normal resistivity logs for borehle diameter and mud resistivity, U.S. Geological Survey Open-File Report 78-669, 12 p.

U. South Carolina, 1992, Sedimentology and stratigraphy of the Upland Unit, SCUREF Cooperative Agreement, Task Order No. 53, Progress Report, Dec. 2.

Table 2. Well location and Plate number, MSB-series of holes.			
MSB wells	East	North	Plates
01B	48483.2	101833.0	4, 6
02B	48748.2	101997.9	4, 6
04B	48312.8	101978.3	4, 6
15B	48818.5	102953.2	4, 7
17BB	46220.8	102009.5	5, 6
21TA	47218.2	103980.9	2
23TAR	49225.8	104298.8	2, 7
26AA	48941.7	104612.8	2
31BB	50067.9	101983.1	4, 6
48C	54077.0	107917.5	1
49A	45864.6	99759.0	5, 7
53B	54574.3	106443.6	1
55C	52029.7	108324.6	1
62B	47906.8	101865.3	5, 6,7
66TA	51096.7	105842.6	1, 7
67B	51989.6	106842.0	1, 7
68B	52308.5	106744.9	1
69TA	52418.4	107772.5	1, 7
71B	44054.7	103801.6	2
72B	48350.3	96387.6	5
73B	45694.0	99270.3	5
75B	48875.5	98937.4	5
76C	45344.0	103061.0	2
82C	51949.4	107521.9	1
83C	52384.7	108405.3	1
84C	51973.7	108967.9	1
85C	53151.4	107835.2	1

Table 3. Well location and Plate number, MHT-series of holes.			
MHT wells	East	North	Plates
01c	48765.6	102706.8	3
02c	48780.3	102747.1	3
03c	48861.1	102704.3	3
04c	48863.5	102778.9	3
05c	48905.9	102725.1	3
06c	48900.0	102810.8	3
07c	48977.5	102788.9	3
08c	48970.2	102880.7	3
09c	49015.6	102814.4	3
10c	49011.6	102892.3	3
17c	48706.9	102394.6	3, 7
18c	48650.9	102486.1	3
19c	48699.1	102502.7	3
20c	48710.8	102589.3	3

Table 4. Location and Plate number for cone penetrometer logs acquired by Applied Research Associates during June - July, 1992.

CPT number	East	North	Plate
1-	48761.5	104527.3	2
2-	47884.8	104243.6	2
3-	45819.4	103251.7	2
4-	45512.1	104120.5	2
5-	47863.3	103874.7	2
6-	48469.7	103064.8	4
7-	47586.2	102444.4	5
9-	47696.7	100993.0	5, 7
10-	46714.6	100505.8	5, 7
11-	46114.5	101349.2	5
12-	45036.4	103267.6	2
13a	45297.1	103066.8	2
13b	45312.2	103083.2	2
14-	46433.0	102736.3	2
15a	48778.9	102963.8	4
15b	48785.4	102957.8	not plotted
17-	50104.1	101955.2	4, 6
18a	48487.1	102198.8	4
18b	48511.1	102232.2	4
19a	48257.9	102264.5	4
19b	48250.5	102268.8	not plotted
20a	47921.3	102448.2	5
20b	47906.8	102500.2	5
21-	48590.5	101383.0	5
22-	48316.8	102495.9	4
23a	46704.5	103862.0	2
23b	46596.2	103812.5	2

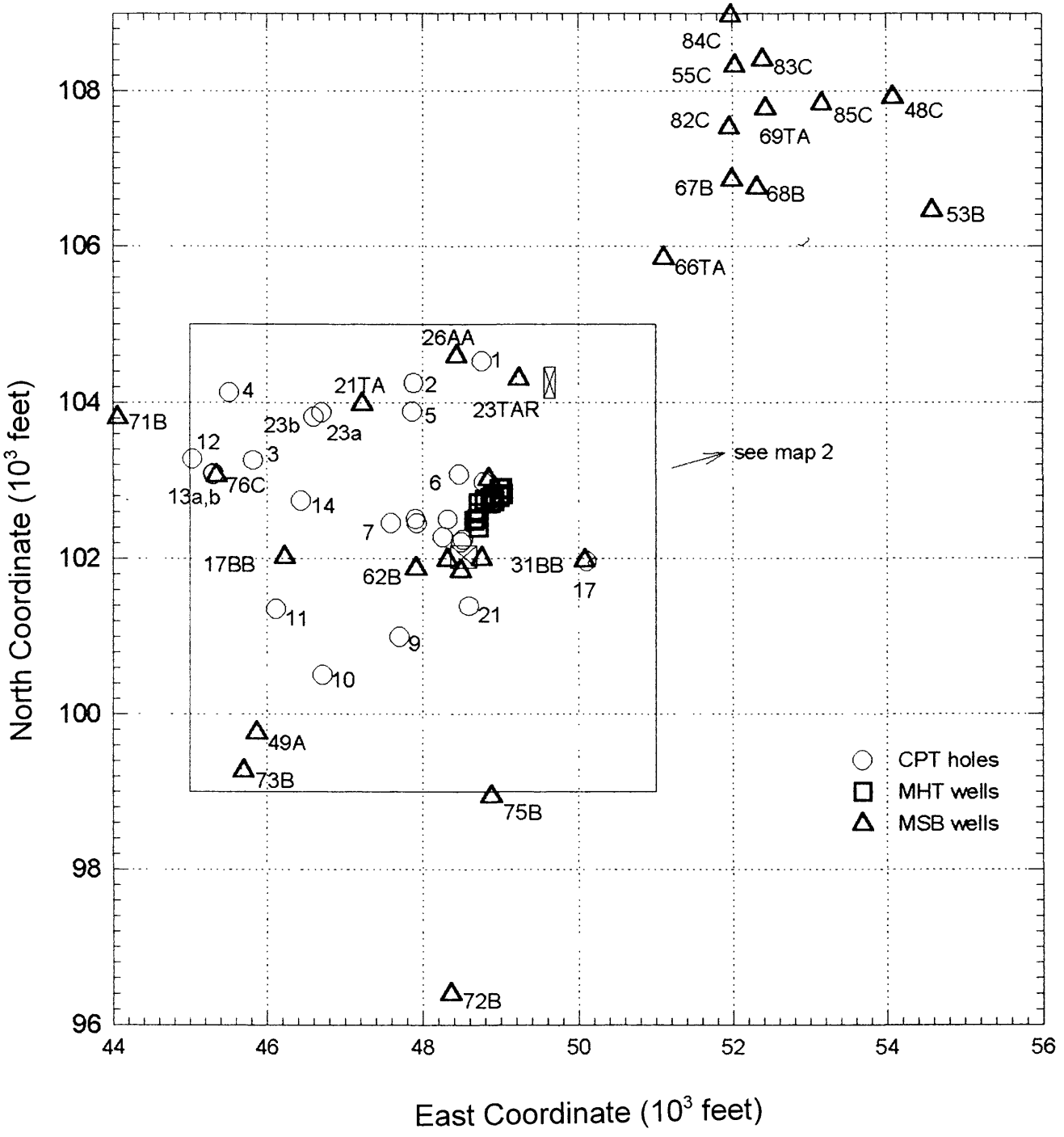

Figure 1. Map of A/M Area showing locations of cone penetrometer (CPT) holes, MHT-series of wells, and MSB-series of wells. Square with X just left of center is the Settling Basin. Rectangle with X just north of center is Building 321-M. All locations with resistivity logs are shown on this map. Names of unlabelled locations are shown on expanded views in Figures 2 and 3.

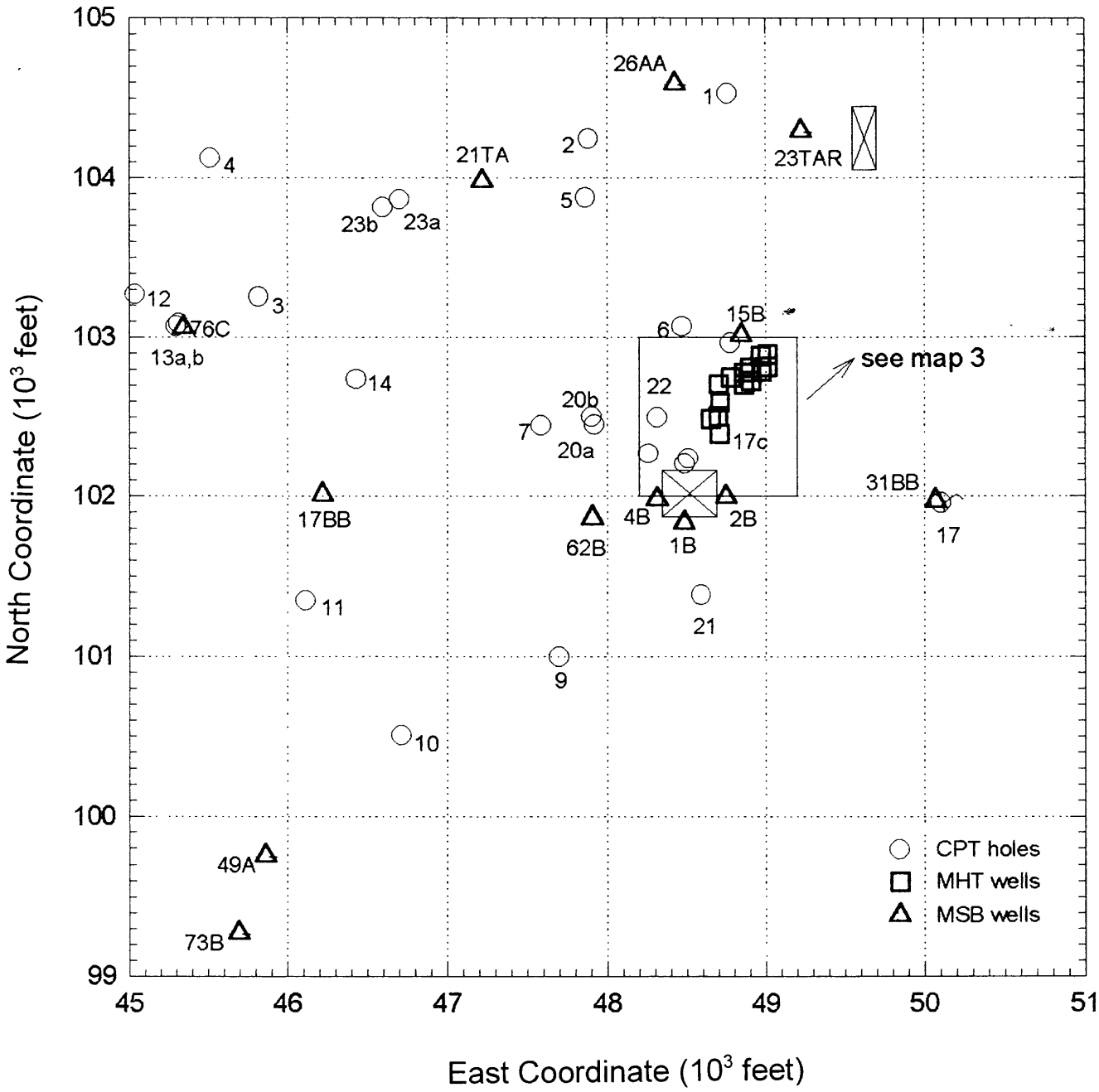

Figure 2. Expanded map (map 2 of Figure 1) within A/M Area showing locations of wells and penetrations. Square with X shows the Settling Basin. Rectangle with X designates Building 321-M.

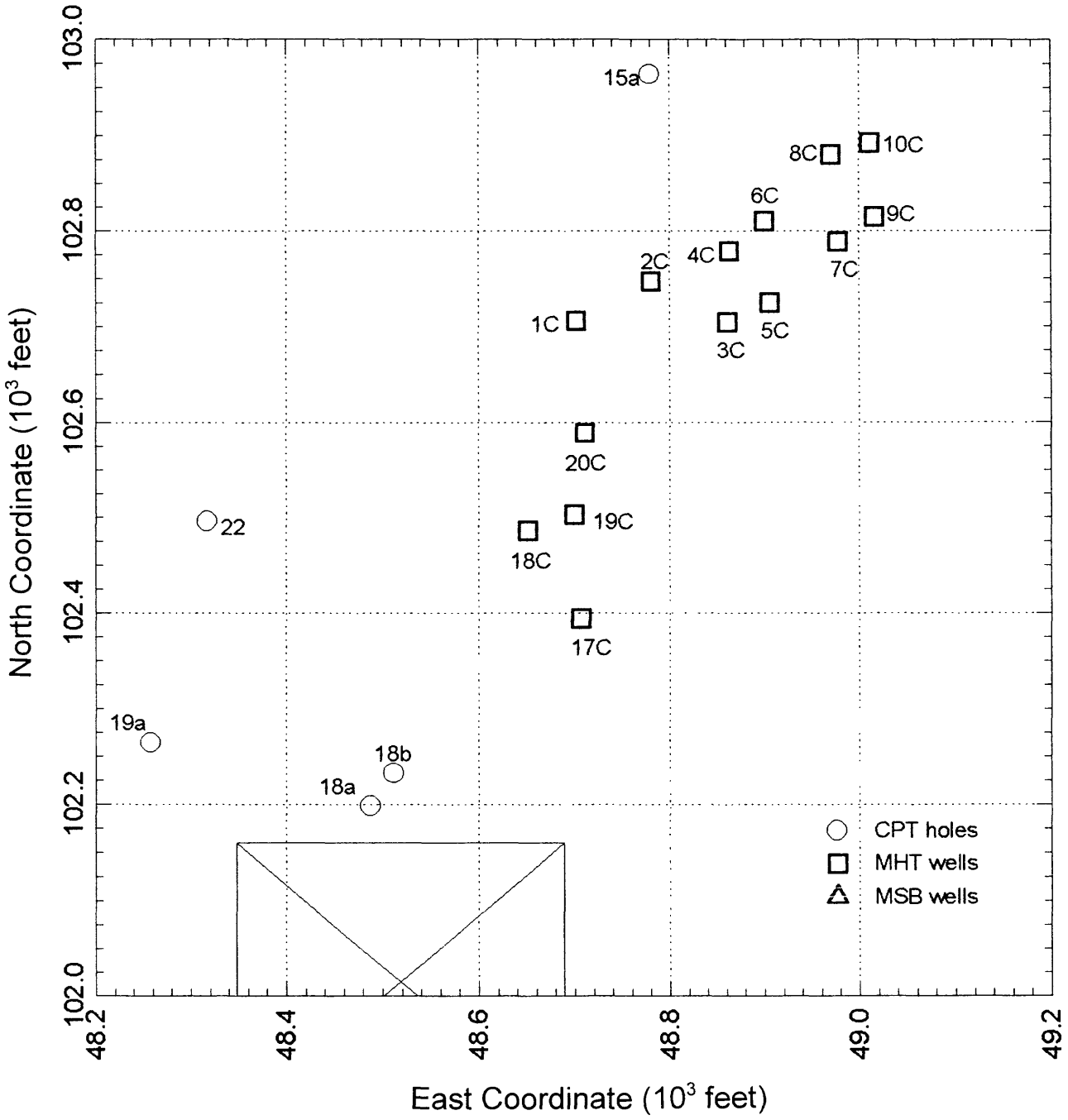

Figure 3. Expanded map (map 3 in Figure 2) north of Settling Basin showing locations of wells and penetrations. Truncated square with X shows northern portion of Settling Basin.

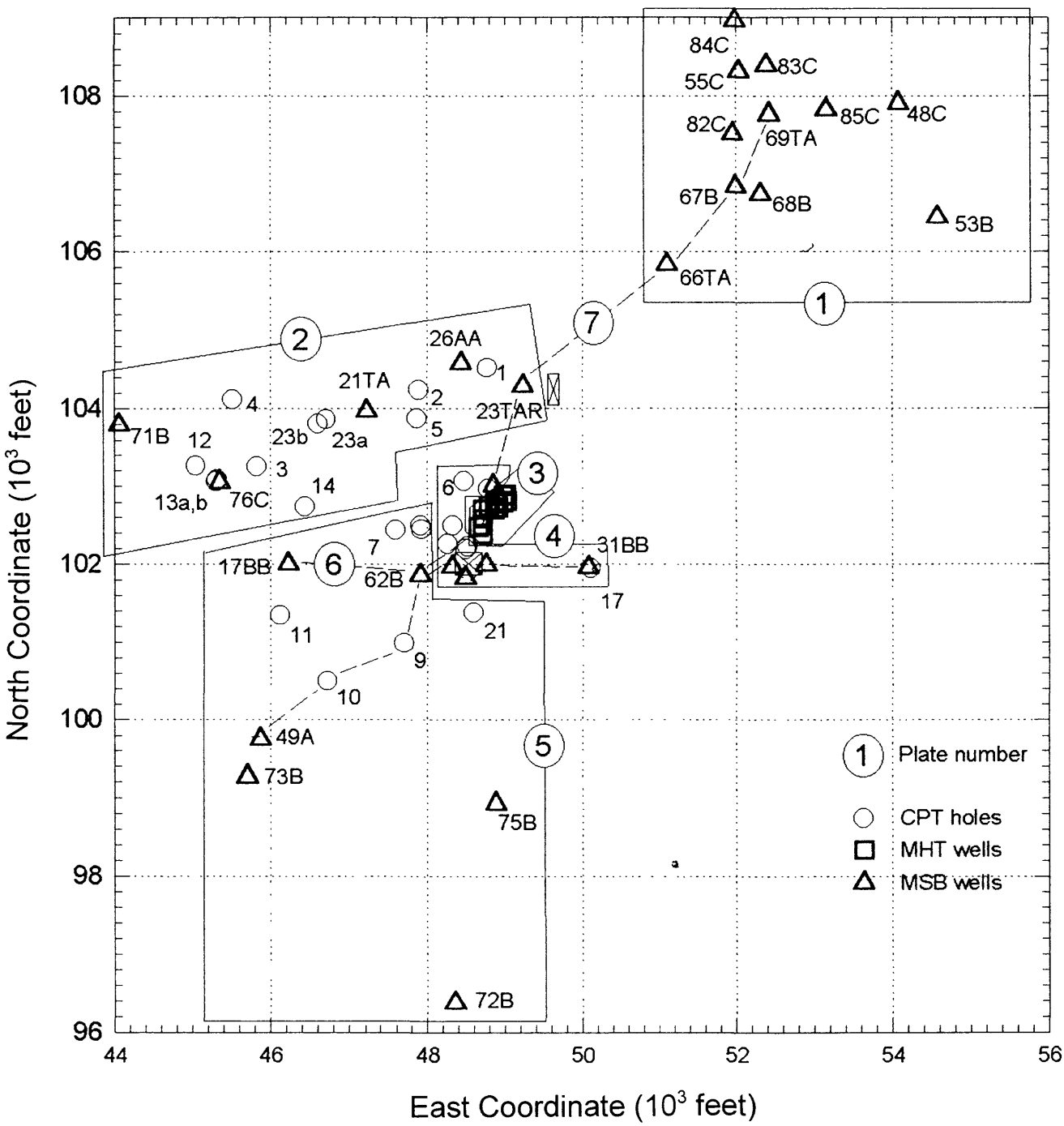

Figure 4. Map of A/M Area showing groups and lines of wells and penetrations for Plates 1 through 7. Grid coordinates are in thousands of feet.

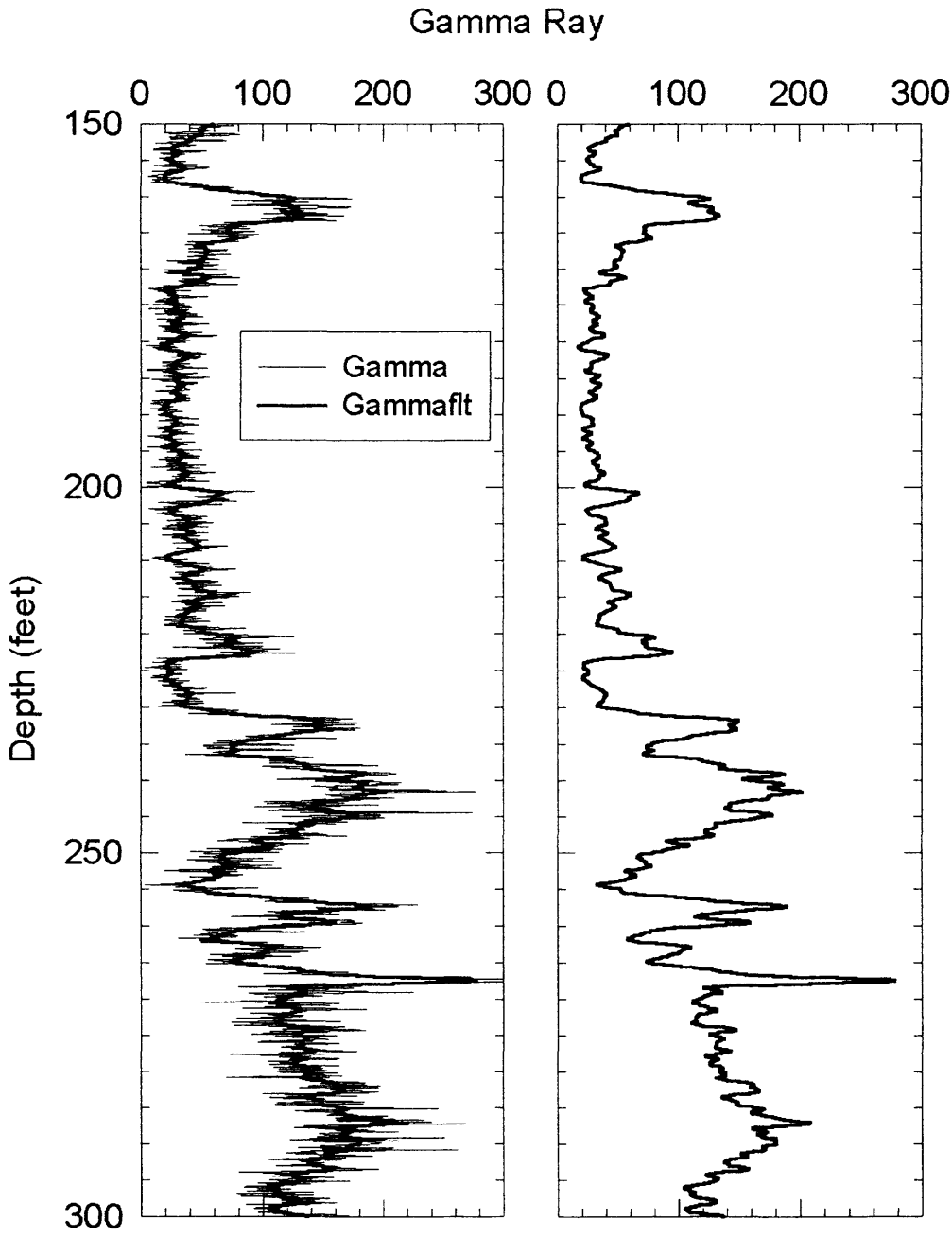

Figure 5. Filtering of gamma-ray log using an 11-point triangular filter. The unfiltered trace is superposed on the filtered trace on the left; the filtered trace is shown individually on the right.

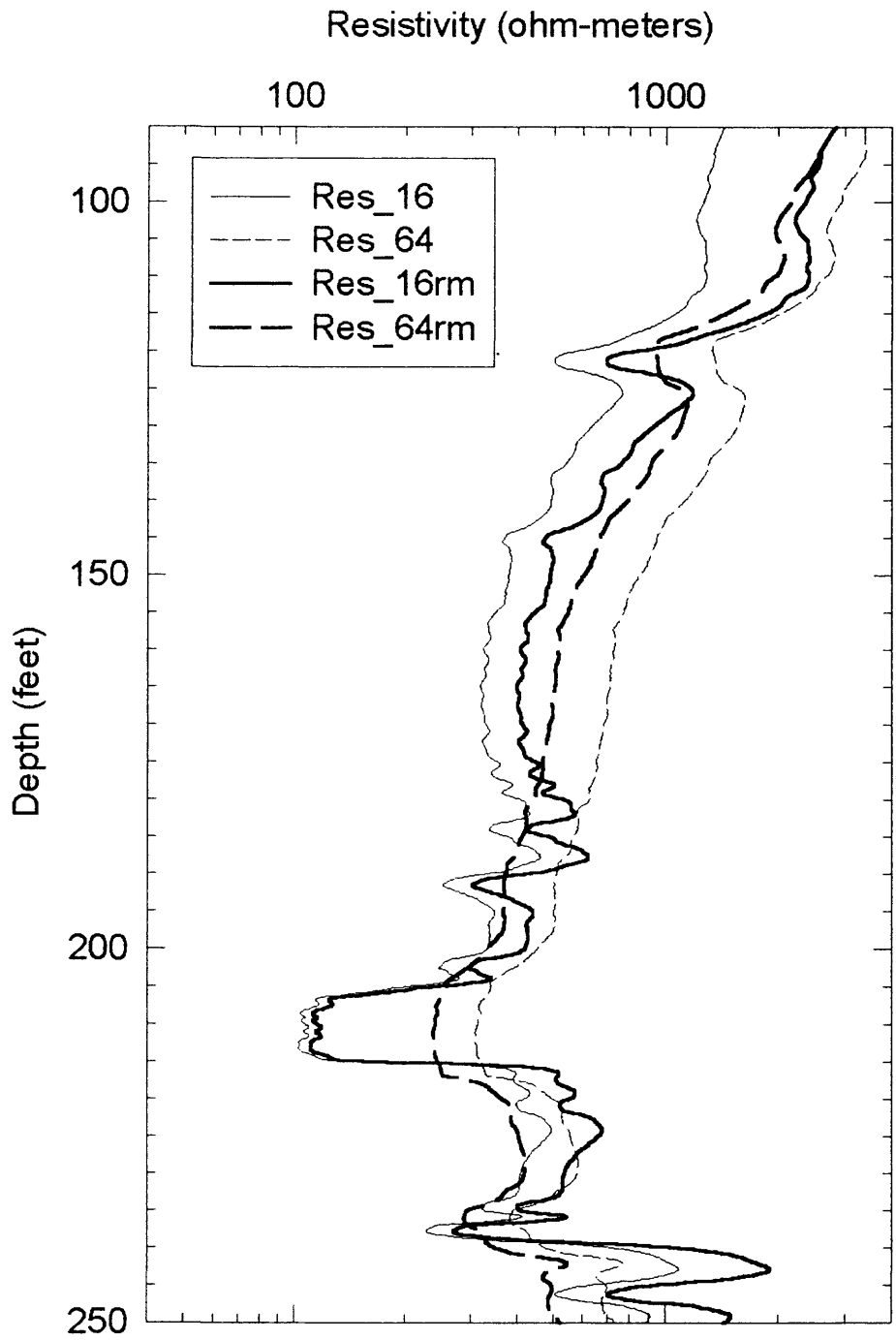

Figure 6a. Short (16-inch) and long (64-inch) normal resistivity logs, before (light traces) and after (dark traces) correction for borehole diameter and fluid resistivity. Example is from well MSB-17BB, drilled with a 12-inch bit.

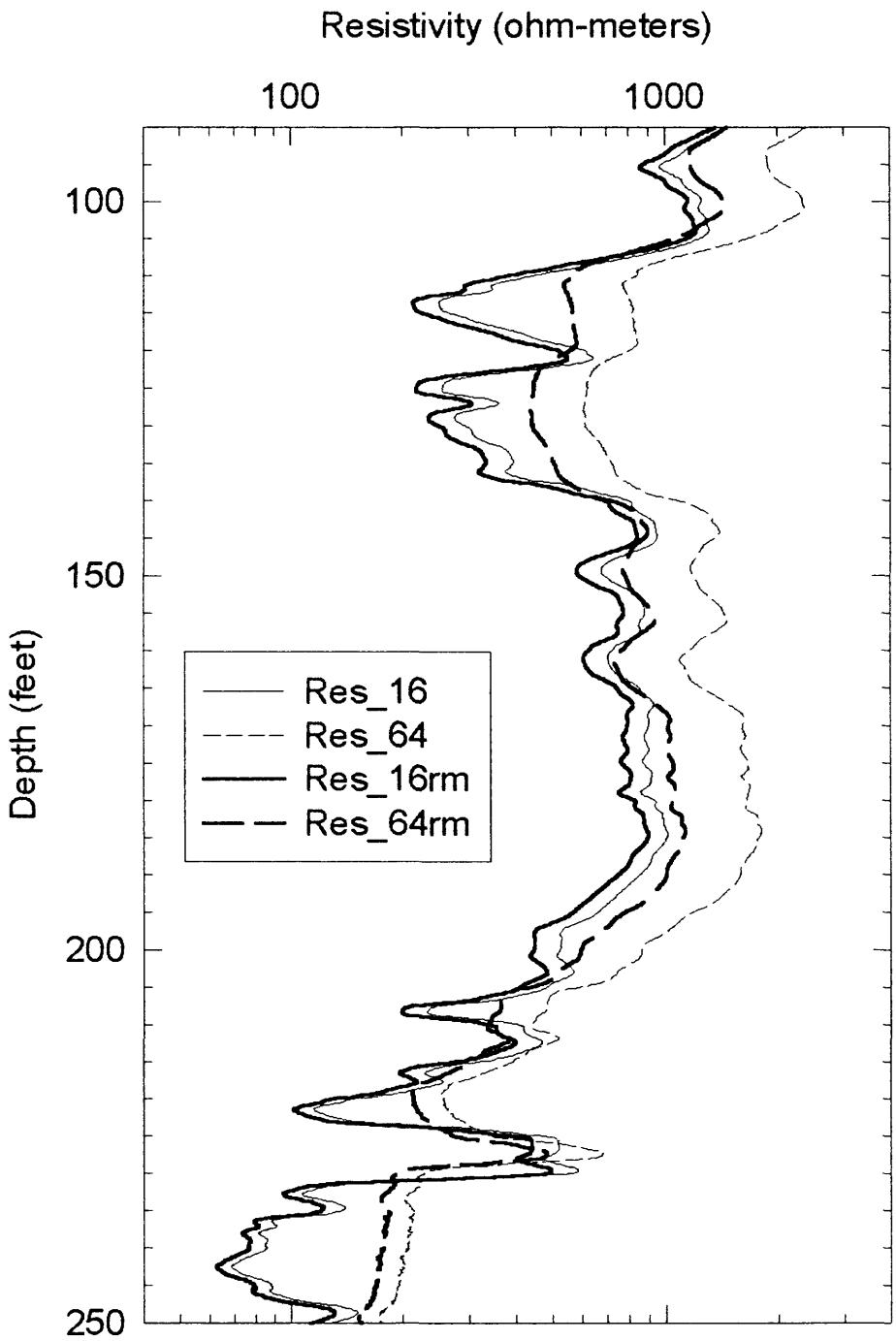

Figure 6b. Short (16-inch) and long (64-inch) normal resistivity logs, before (light traces) and after (dark traces) correction for borehole diameter and fluid resistivity. Example is from well MSB-26AA, drilled with a 5-inch bit.

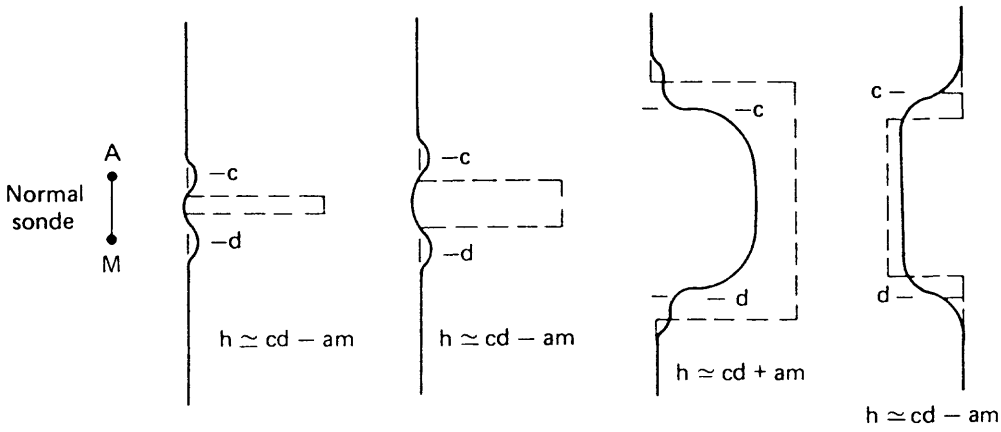

Figure 7. Apparent resistivity log from a two-electrode array (solid curve) in. Electrode spacing is represented by short line "A-M". Case 1 (left) and case 2: resistive bed is thinner than electrode spacing. Case 3: resistive bed is thicker than electrode spacing. Case 4 (right): conductive bed is thicker than electrode spacing. Points cd are changes in curvature on the logs from which bed thickness must be inferred. From Hearst and Nelson (1985), after Guyod (1944).

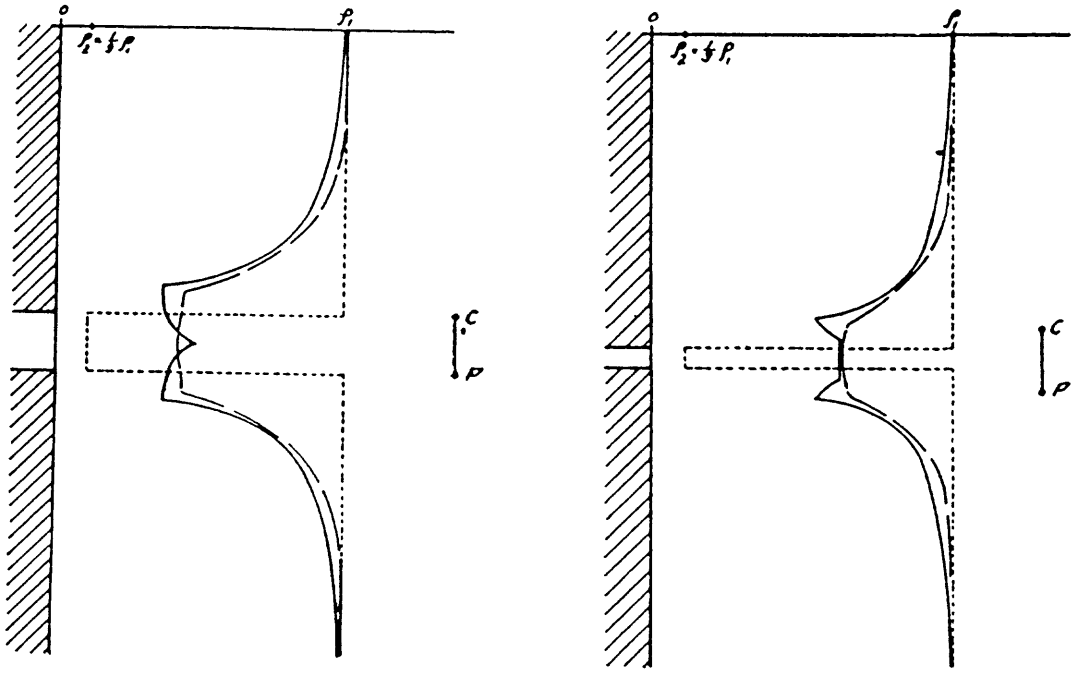

Figure 8. Two-electrode resistivity logs (solid and long dash curves) in formations having resistivity values indicated by the dotted lines. Resistivity of the center bed is equal to 1/9 the resistivity of the surrounding beds. Electrode array is represented by short line "C-P". Bed thickness is comparable to the electrode spacing (left) and one-third the electrode spacing (right). Solid curves are computed with no borehole fluid. Dashed curves assume that a borehole fluid is present. From Guyod, 1944.

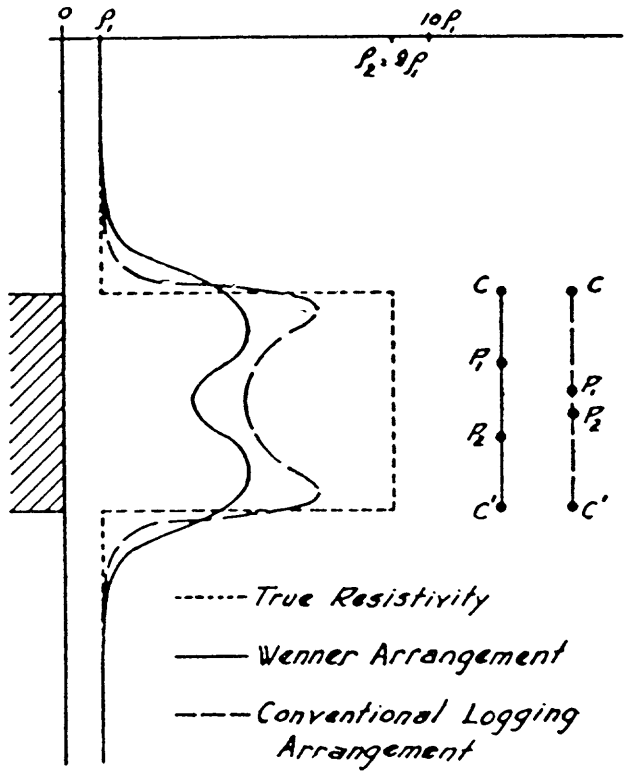

Figure 9. Apparent resistivity from a Wenner array (solid) and from a four-electrode array (long dash) in a bed with resistivity 9 times greater than that of surrounding beds. True resistivity of beds is indicated by short dashed line. From Guyod, 1944.

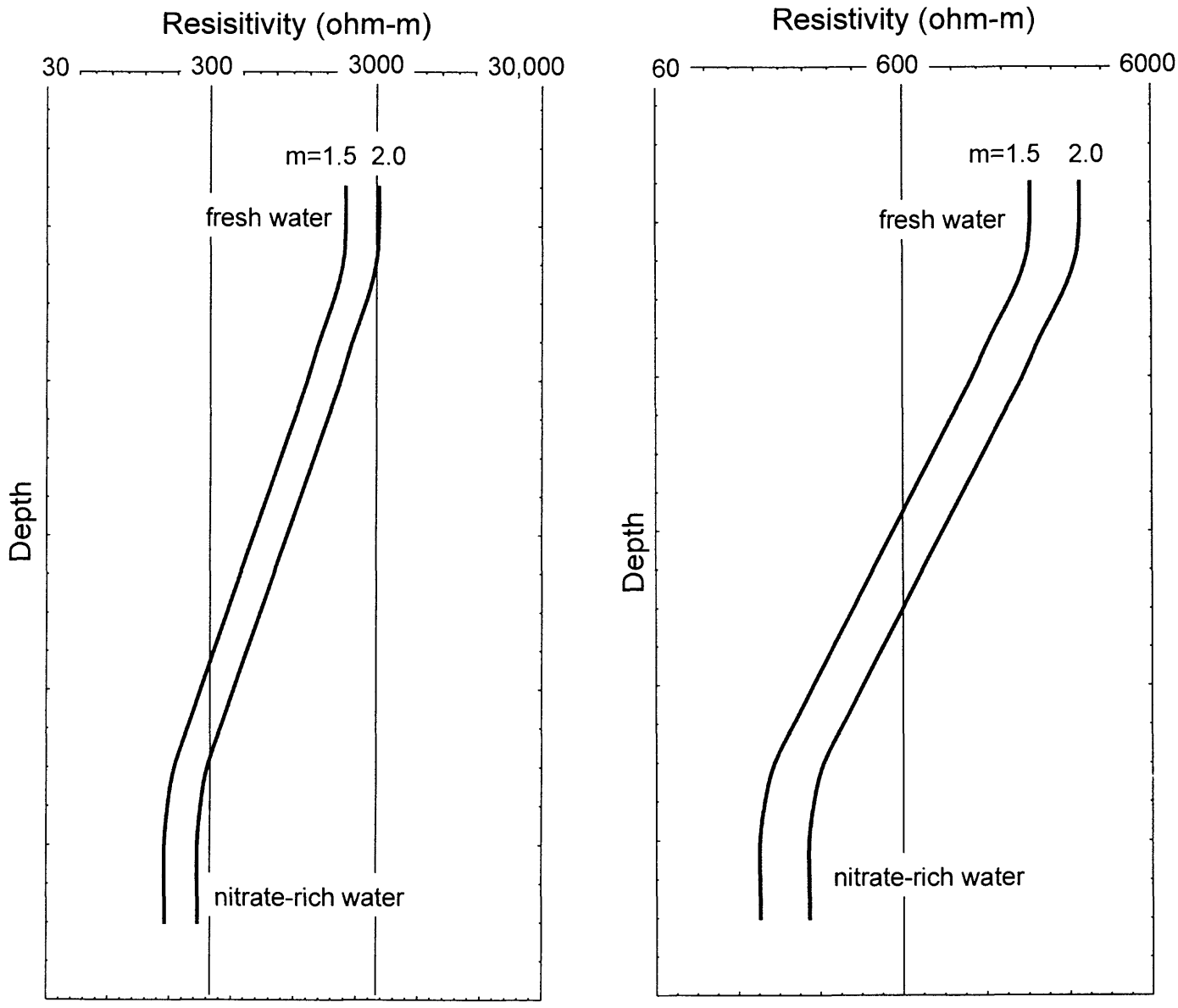

Figure 10. Hypothetical resistivity log in sand of 40% porosity. Formation water is fresh at top of log, gradually becoming more nitrate rich to the bottom of log. The two curves represent the uncertainty due to lack of data on the cementation exponent, *m*. Scales are for cone penetrometer (left) and for open-hole logs (right), as scaled on the Plates.

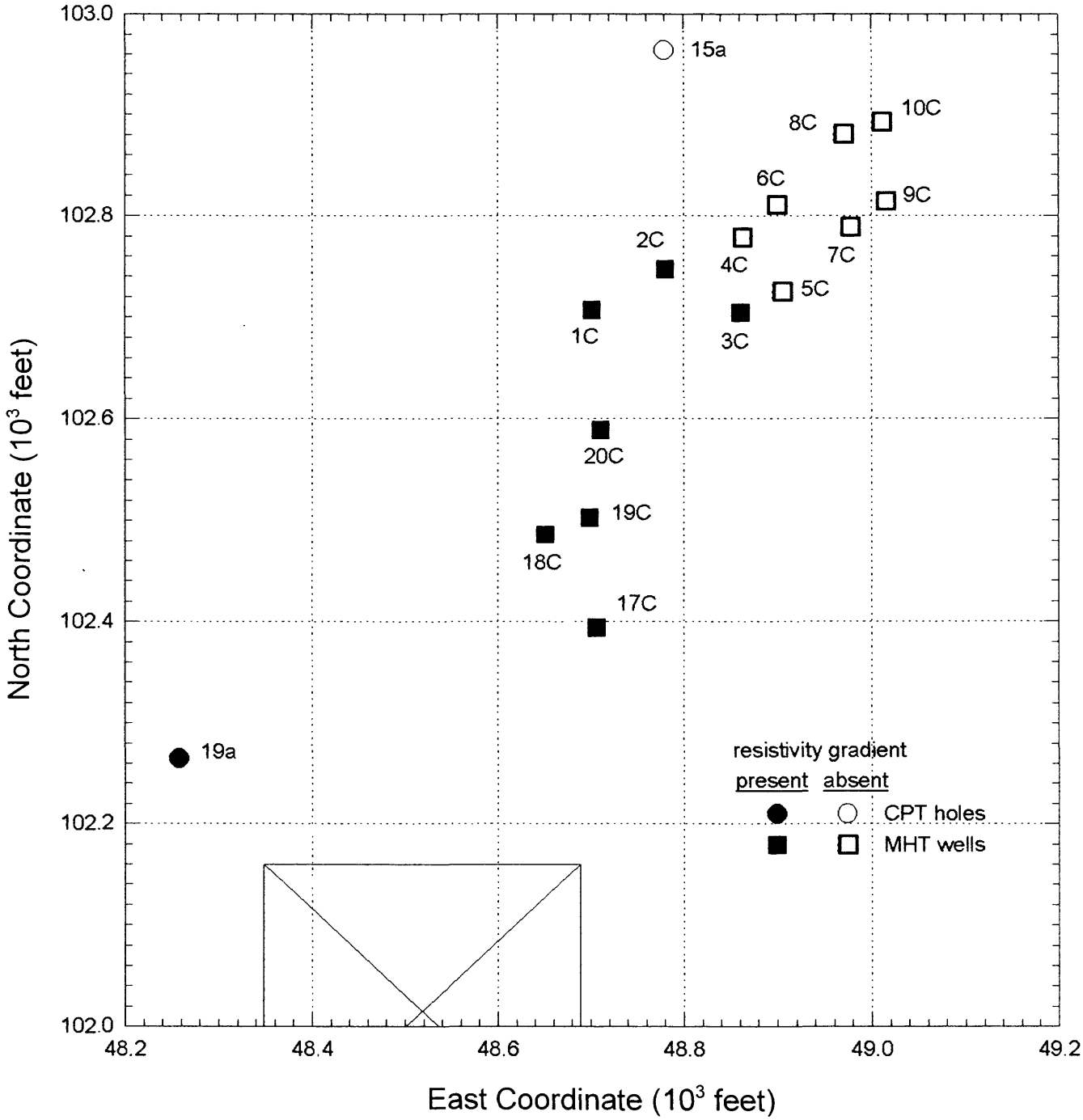

Figure 11. Presence of resistivity gradient in area just north of Settling Basin. Well and penetration symbols made solid if a resistivity gradient is present below the water table. If the water table was not reached, then no symbol is shown. Map boundaries same as Figure 3.

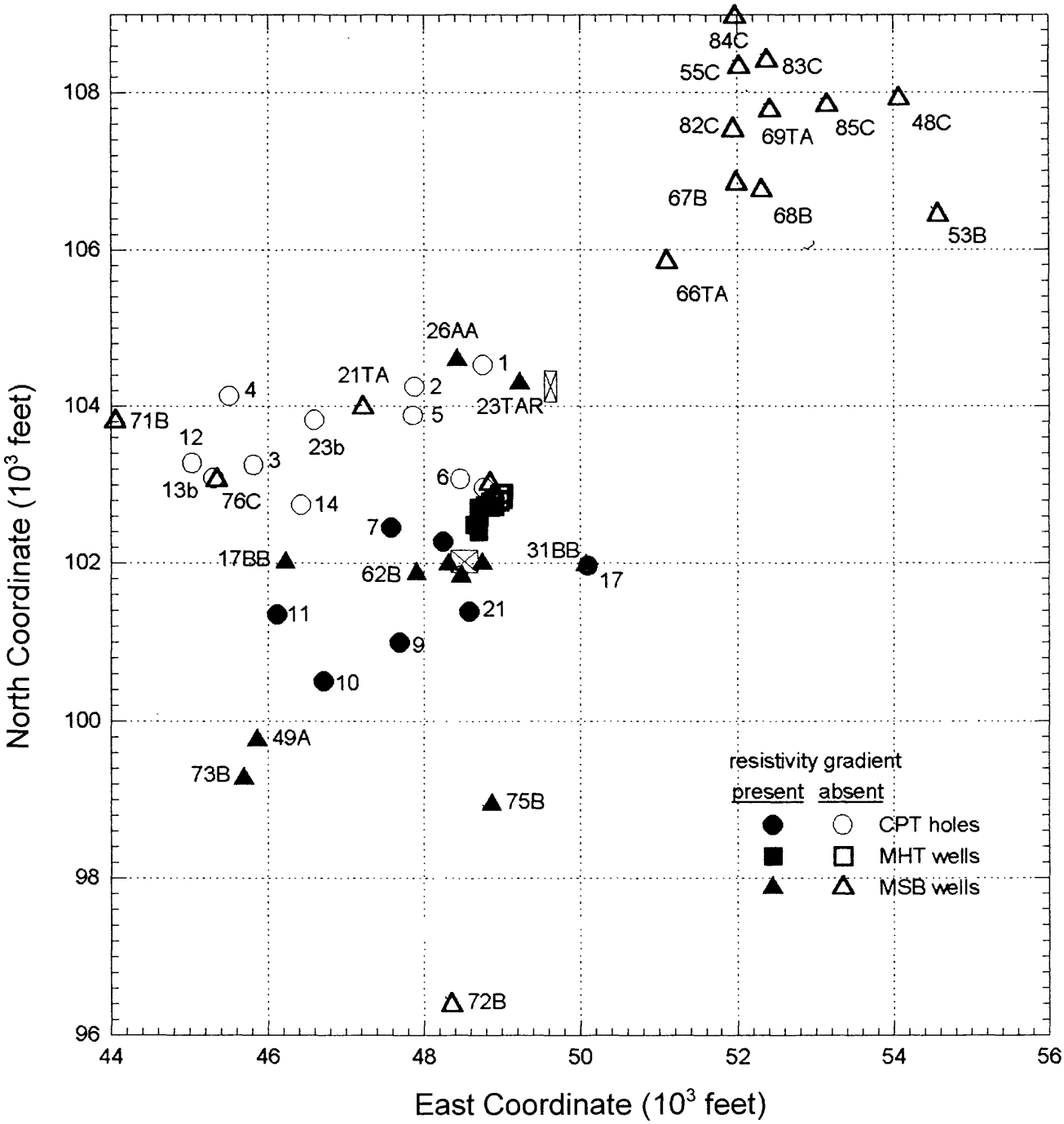

Figure 12. Presence of resistivity gradient on map of A/M area. Well and penetration symbols are solid if a resistivity gradient is present below the water table. If the water table was not reached, then no symbol is shown. Map boundaries same as Figure 1.